Robust PID Design by Chance-Constrained Optimization

Mercader, Pedro; Soltesz, Kristian; Baños, Alfonso

Published in:
Journal of the Franklin Institute

DOI:
10.1016/j.jfranklin.2017.10.017

2017

Document Version:
Peer reviewed version (aka post-print)

Robust PID Design by Chance-Constrained Optimization

Pedro Mercader[1,*], Kristian Soltesz[2], and Alfonso Baños[1]

[1]Department of Computer and Systems Engineering, University of Murcia, Spain
[2]Department of Automatic Control, Lund University, Sweden

[*]Corresponding author: pedro.mercader@um.es

Abstract

A method for synthesizing proportional–integral–derivative (PID) controllers for process models with probabilistic parametric uncertainty is presented. The proposed method constitutes a stochastic extension to the well-studied maximization of integral gain optimization (MIGO) approach, i.e., maximization of integral gain under constraints on the $\mathcal{H}_\infty$-norm of relevant closed-loop transfer functions. The underlying chance-constrained optimization problem is solved using a gradient-based algorithm once it has been approximated by a deterministic optimization problem. The approximate solution is then probabilistically verified using randomized algorithms (RAs). The proposed method is demonstrated through several realistic synthesis examples.

1 Introduction

Designing a control system comprises a trade-off between achieving a good performance level and guaranteeing adequate stability margins. Model uncertainty should be taken into account in the problem formulation, since the parameters of the process are seldom known exactly during the modeling phase, or they usually change as the environment or the operation point changes. When model uncertainty is explicitly incorporated into the problem formulation, it impacts the achievable performance level. Most of the robust control literature (e.g. QFT, $\mathcal{H}_\infty$, interval methods, etc.) deals with deterministic uncertainty descriptions [1], resulting in worst-case specifications for performance and robustness. It is well-known that a deterministic approach may potentially lead to conservative designs, since the occurrence of the worst-case scenario may be very unlikely.

The robust design of PID controllers is usually stated as a constrained optimization problem (see [2, 3])

$$\begin{aligned} \underset{\mathbf{k}}{\text{minimize}} \quad & J(\boldsymbol{\theta}, \mathbf{k}) \\ \text{subject to} \quad & \boldsymbol{\varphi}(\boldsymbol{\theta}, \mathbf{k}) \leq \mathbf{0}, \end{aligned} \tag{1}$$

where $\mathbf{k}$ is the design (controller) parameter vector, and $\boldsymbol{\theta}$ is a deterministic vector of process model parameters. The rationale of the problem (1) is that minimization of the objective J aims at maximizing performance over $\mathbf{k}$, while the constraint vector $\boldsymbol{\varphi}$ (with components φ_i, and $\leq$ corresponding to the component-wise inequality) is in place to ensure robustness (i.e. to guarantee adequate stability margins).

If the model parameter vector $\boldsymbol{\theta}$ is instead assumed to be a random variable, the cost function $J(\boldsymbol{\theta}, \mathbf{k})$ and the constraints $\boldsymbol{\varphi}(\boldsymbol{\theta}, \mathbf{k})$ also become random variables. A possible extension of (1), taking this into account, is formulated as the chance-constrained optimization problem

$$\begin{aligned} \underset{\mathbf{k}}{\text{minimize}} \quad & \mathbb{E}[J(\boldsymbol{\theta}, \mathbf{k})] \\ \underset{\forall i}{\text{subject to}} \quad & \Pr[\varphi_i(\boldsymbol{\theta}, \mathbf{k}) \leq 0] \geq 1 - \alpha_i. \end{aligned} \tag{2}$$

where $\alpha_i \geq 0$ specify permissible probabilities of constraint violation. The formulation (2) aims to minimize the expected cost, subject to a fulfillment of the constraints with at least a predefined level of probability. The use of a probabilistic uncertainty model enables computation of constraint violation probabilities; in

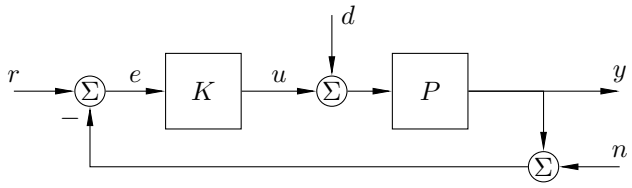

Figure 1: Feedback control system, consisting of process P and controller K. Signals are: process output y, controller output u, load disturbance d and output disturbance (noise) n.

this way, higher performance levels may be achieved while maintaining the probability of constraint violation below a certain value – typically small, and predefined by the user.

The main motivation of the present work has been to obtain a probabilistic extension of to the well-studied maximization of integral gain optimization (MIGO) approach [2]. Focus lies on presenting a numerically efficient approach. Early work focusing on robustness constrained IE minimization was presented in [2]. Efficient convex-optimization-based algorithms for solving the same problem were recently presented in [4], and extended to design problems involving QFT specifications in [5]. Robustness constrained minimization of IAE has been investigated in [6]. Efficient gradient-based algorithms for the same problem were proposed [7]. Simultaneous synthesis of PID controllers and measurement filter was addressed in [8]. It is worth to notice that stability constraints used in the MIGO approach are not convex [8], hence all these methods calculate a local optimum. The method presented here faces the same limitation.

Related prior works that combine PID and probabilistic modeling are briefly presented below: In [9], a Taylor series approximation was used to deal with the expectation integrals. Test-points methods were proposed in [10] to approximate these integrals in the context of PID control and integrated into an autotuner method in [11]. In [12], a polynomial chaos approach was applied to optimize temporal responses. The work [13] considers the design of decentralized (multivariable) PID controllers with probabilistic robustness via Monte Carlo (MC) simulations and genetic algorithms (GAs). Finally, other applications of stochastic methods to the design of PID controllers, not necessarily for process models with probabilistic parameterization, have been reported, for example, in [14, 15, 16].

This work is organized as follows: The problem formulation is given in Section 2. An approach to approximately solve the resulting chance-constrained optimization problem is presented in Section 3. Randomized algorithms for numerical verification are presented in Section 4. Examples are given in Section 5, and finally, a summary and conclusions are presented in Section 6.

2 Problem statement

We consider the feedback control system shown in Fig. 1, with process P and controller K. The process model is given by the arbitrary-order time-delayed transfer function

$$P(s,\boldsymbol{\theta}) = \frac{b_B s^B + b_{B-1}s^{B-1} + \cdots + b_0}{a_A s^A + a_{A-1}s^{A-1} + \cdots + a_0} e^{-hs}, \tag{3}$$

where A and B are known constants satisfying $B \leq A$, and

$$\boldsymbol{\theta} = [b_B, b_{B-1}, \ldots, b_0, a_A, a_{A-1}, \ldots, a_0, h]^\top \tag{4}$$

is the stochastic process model parameter vector. The joint PDF of $\boldsymbol{\theta}$ will be denoted $f(\boldsymbol{\theta}) : \mathbb{R}^n \mapsto \mathbb{R}$, where $n = A + B + 3$. A multivariate uniform PDF is assumed, being the probabilistic counterpart of the (unknown-but-bounded) interval parametric uncertainty. A rigorous justification for the use of the uniform PDF in this setting is done in [17].

The controller considered in this work is a filtered PID with the following structure

$$K(s,\mathbf{k}) = \frac{k_p + \dfrac{k_i}{s} + k_d s}{1 + sT_f + s^2 T_f^2/2}, \tag{5}$$

where $\mathbf{k} = [k_p, k_i, k_d, T_f]^\top$ is a deterministic vector of its parameters.

The control design problem is formulated as a constrained optimization problem, in the spirit of the chance-constrained optimization problem (2). Load disturbance attenuation is optimized subject to robustness constraints. (Tracking could be improved by using a two-degrees-of-freedom (2-DOF) control structure, with a reference pre-filter [3].) Two well-known ways of achieving disturbance rejection, are the minimization of either the *integrated error* (IE)

$$\mathrm{IE}(\boldsymbol{\theta}, \mathbf{k}) = \int_0^\infty e(t, \boldsymbol{\theta}, \mathbf{k}) dt, \tag{6}$$

or the *integrated absolute error* (IAE)

$$\mathrm{IAE}(\boldsymbol{\theta}, \mathbf{k}) = \int_0^\infty |e(t, \boldsymbol{\theta}, \mathbf{k})| \, dt. \tag{7}$$

The error e in both (6) and (7) is caused by a unit load disturbance step d, applied with the control system in an equilibrium state, see Fig. 1.

These two performance measures are very similar for well-damped closed-loop systems. It is important to note that enforcing robust stability ensures well-damped closed-loop system. A decisive factor to consider minimization of IE in favor of IAE is that that minimization of IE is equivalent to maximization of k_i in (5) (for processes with positive steady-state gain) [2]. That is, IE minimization results in a convex objective, that, in addition, does not depend on process parameters, and thus takes a deterministic value. Unfortunately this is not the case for the IAE. Nevertheless, the same approach presented here could be applied when using the IAE as objective, see [10].

In this work we combine (2) with the IE objective (6) expressed as maximization of k_i and $\mathcal{H}_\infty$-constraints on $S(s, \boldsymbol{\theta}, \mathbf{k}) = (1 + P(s, \boldsymbol{\theta}) K(s, \mathbf{k}))^{-1}$ and $T(s, \boldsymbol{\theta}, \mathbf{k}) = 1 - S(s, \boldsymbol{\theta}, \mathbf{k})$, arriving at the chance-constrained optimization problem

$$\begin{aligned} \underset{\mathbf{k}=[k_p,k_i,k_d,T_f]^\top}{\text{minimize}} \quad & -k_i \\ \text{subject to} \quad & \Pr[\|S(\boldsymbol{\theta}, \mathbf{k})\|_\infty - M_S \leq 0] \geq 1 - \alpha_S, \\ & \Pr[\|T(\boldsymbol{\theta}, \mathbf{k})\|_\infty - M_T \leq 0] \geq 1 - \alpha_T, \end{aligned} \tag{8}$$

where M_S and M_T are greater than 1, and α_S and α_T are nonnegative and less than 1. Under this setting, these specifications have an impact on the loop bandwidth. This should be accounted for when implementing a digital controller, since it is advisable to work with a sampling frequency at $10-20$ times the loop bandwidth.

3 Chance-constrained optimization problem

Our aim is to solve the probabilistic optimization problem (8) in an efficient way, using a gradient-based algorithm, such as sequential quadratic programming (SQP) or interior point methods [18]. This approach relies on numerous evaluations of the objective and constraints, calling for efficient approximations of the multidimensional expectation integrals resulting from the constraint (Section 3.1). The indicator function, used to obtain probability values, has to be approximated by a differentiable function in order to obtain reliable gradient information by numerical differences (Section 3.2). Finally, guidelines to obtain good initialization candidates to be used in the optimization algorithm need to be established (Section 3.3).

3.1 Constraints evaluation

Constraints evaluation implies the calculation of expectation integrals. For example, the probability value of satisfaction for the first constraint of (8) is

$$\Pr[\|S(\boldsymbol{\theta}, \mathbf{k})\|_\infty - M_S \leq 0] = \mathbb{E}\left[\mathcal{I}[\|S(\boldsymbol{\theta}, \mathbf{k})\|_\infty - M_S]\right], \tag{9}$$

where $\mathcal{I}[\cdot]$ is the indicator function, given by

$$\mathcal{I}[x] = \begin{cases} 1, & \text{if } x \leq 0, \\ 0, & \text{if } x > 0. \end{cases} \tag{10}$$

In this section, we introduce a function $g(\boldsymbol{\theta}, \mathbf{k})$, which takes on the role of the argument of the expectation operator. The expectation of $g(\boldsymbol{\theta}, \mathbf{k})$ is defined by the multivariate integral

$$\mathbb{E}[g] = \int_{\Delta} g(\boldsymbol{\theta}, \mathbf{k}) f(\boldsymbol{\theta}) d\boldsymbol{\theta}, \tag{11}$$

where Δ is the support of $f(\boldsymbol{\theta})$, i.e., the set of values for which $\boldsymbol{\theta}$ is nonzero. In general, analytical solution to this type of integral does not exist for non-linear $g(\boldsymbol{\theta}, \mathbf{k})$. Henceforward, the dependence with respect to $\mathbf{k}$ will be omitted, whenever possible, to simplify the notation. Several numerical approaches have been presented in the literature to obtain approximate values of expectation integrals, among others, linearization of the integrand, Monte-Carlo methods, and quadrature rules [19]. In this work, the expectation integral (11) is approximated by a quadrature rule

$$I[g] \equiv \sum_{i=1}^{N} w_i g(\boldsymbol{\theta}_i), \tag{12}$$

comprising nodes $\boldsymbol{\theta}_i$ and weights w_i, $i = 1, \ldots, N$. An important feature of (12) is that nodes and weights depend solely on f. Hence they can be obtained for a given f, and subsequently used for an arbitrary g.

A quadrature rule, such as (12), is said to have *degree of polynomial exactness* D, if it delivers exact integral values, $I[g] = \mathbb{E}[g]$, for any polynomial g of total order at most D[1]. This issue is of utmost importance when using a quadrature rule, since high degree of polynomial exactness translates to good integral approximations whenever g is approximable by polynomial functions (through e.g. Taylor expansion).

We will start presenting the univariate case, and then extend it to its multivariate counterpart.

3.1.1 Univariate quadrature

Consider first the one-dimensional case, i.e., $n = 1$. A sequence of quadrature rules defines, for every $\nu \in \mathbb{N}$ (*accuracy level*), a set of N_ν nodes $\theta_{\nu,i}$ and weights $w_{\nu,i}$, $i = 1, \ldots, N_\nu$, which are used to approximate the expectation integral (11) as the following weighted sum

$$I_\nu[g] \equiv \sum_{i=1}^{N_\nu} w_{\nu,i} g(\theta_{\nu,i}). \tag{13}$$

Here, the degree of polynomial exactness is denoted D_ν, since it depends on the accuracy level ν. A well-known example is the sequence of Gauss-Legendre (GL) quadrature rules. It comprises $N_\nu = \nu$ nodes and achieves the maximum possible degree of polynomial exactness, $D_\nu = 2\nu - 1$ [19]. An interesting class of sequences of quadrature rules is the class of nested quadrature rules. For these, the set of nodes used for a given accuracy is a subset of the nodes used for any higher accuracy. These sequences are of interest when extending to the multivariate case. Herein, the delayed sequence of the Kronrod-Patterson (dKP) nested quadrature rules will be used, see [20].

3.1.2 Multivariate quadrature

The extension from univariate to multivariate quadrature can be achieved using the tensor product

$$\left(I_{\nu_1} \otimes \cdots \otimes I_{\nu_n}\right)[g] \equiv \sum_{i_1=1}^{N_{\nu_1}} \cdots \sum_{i_n=1}^{N_{\nu_n}} w_{\nu_1,i_1} \cdots w_{\nu_n,i_n} g\left(\left[\theta_{\nu_1,i_1}, \ldots, \theta_{\nu_n,i_n}\right]^\top\right). \tag{14}$$

This is referred to as full grid, as opposed to sparse grid, which will be presented later. The degree of exactness of (14) is the same as the minimum degree of exactness of the underlying univariate quadratures. The main drawback is that it exhibits an exponential growth of nodes with respect to the dimension n (it

[1]The total order of a polynomial is defined as the maximum total order of its monomials, and the total order of a monomial is defined as the sum of orders with respect to the individual variables. For example, a 2-dimensional polynomial of total order 2 may contain terms as θ_1, θ_2, θ_1^2, θ_2^2, and $\theta_1\theta_2$.

suffers from a *curse of dimensionality*). This is due to the quadrature rule not being exact in a class of polynomials of a bounded total order, but for a tensor product of univariate polynomials [21][2].

An alternative to the full grid is available through Smolyak's product [22]. The Smolyak product rule of accuracy level q, for n-dimensional integration, was formulated in [23] as

$$S_{q,n}[g] = \sum_{q+1 \leq \|\boldsymbol{\nu}\|_1 \leq q+n} (-1)^{q+n-\|\boldsymbol{\nu}\|_1} \binom{n-1}{\|\boldsymbol{\nu}\|_1 - \nu - 1} (I_{\nu_1} \otimes \cdots \otimes I_{\nu_n})[g], \tag{15}$$

where $\boldsymbol{\nu} = [\nu_1, \ldots, \nu_n]^\top$. This rule consists of a weighted sum of product rules of accuracy levels defined by $\boldsymbol{\nu}$. Bounds on $\|\boldsymbol{\nu}\|_1$ imply that if a high level of accuracy is used in one dimension, relatively low accuracy levels are used in the others.

Two important properties of the Smolyak's product rule regarding degree of polynomial exactness and dimensional complexity are stated below (see [19] for a more detailed exposition):

- Assume that the sequence of univariate quadrature rules I_ν, with $\nu \in \mathbb{N}$, is exact for all univariate polynomials of order $2\nu - 1$. Then, the Smolyak product rule $S_{q,n}$ is exact for n-variate polynomials of total order $2q - 1$ or less.
- The number of nodes grows polynomially with respect to the dimension n, as opposed to the exponential growth of the full grid (14).

Both sequences of univariate quadrature rules presented here, GL and dKP, satisfy the previous assumption on polynomial exactness degree.

Nested quadrature rules (such as dKP), which are usually less efficient in the univariate case, become attractive when combined with Smolyak's product, since the nested quadrature rules make the union of the tensor products in (15) a much smaller set than when using a non-nested quadrature rule.

3.2 Constraint gradient evaluation

Gradient-based algorithms use the objective and constraint gradients with respect to the controller parameter vector, to find a (local) minimum to the optimization problem (8). The gradient of the objective function is trivial; on the other hand, the gradient of the constraints requires more attention. An analytic expression for the constraint gradients is generally not available. They may be approximated by finite differences, but the combination of the (non-smooth) indicator function with the quadrature rule does not provide reliable gradient information. Several differentiable functions have been suggested as smooth approximations of the indicator function, including the sigmoid

$$\sigma_a(x) = \frac{1}{1 + e^{ax}}, \tag{16}$$

where $a \geq 0$. This is a smooth and tight approximation (it tightens as a increases), used in several other applications [24]. The use of approximations (quadrature rule and sigmoid function) calls for verification of numeric results. This is the topic of Section 4.

3.3 Selection of initial points

To solve the chance-constrained optimization problem (8), a feasible initial point has to be provided to the gradient-based algorithm. Controller parameters with the three first components equal to zero and a stable filter (i.e. $\mathbf{k} = [k_p, k_i, k_d, T_f]^\top = [0, 0, 0, T_f]^\top$ where $T_f \geq 0$) satisfy the constraints for any asymptotically stable process. Otherwise, a stabilizing and feasible initial controller candidate has to be found [4].

The solution of the deterministic counterpart of the considered probabilistic design problem is an appealing alternative to the zero controller. In addition to being feasible, the corresponding controller is associated with a lower objective. This translates to a faster convergence of the method using to solve the optimization problem.

[2]For example, considering $n = 2$ and $D = 2$, in addition to the polynomials θ_1, θ_2, $\theta_1\theta_2$, θ_1^2, and θ_2^2, it is also exact for polynomials involving the higher-order terms $\theta_1^2\theta_2$, $\theta_1\theta_2^2$, and $\theta_1^2\theta_2^2$.

4 Probabilistic verification

It is of particular interest to investigate how the approximations involved in solving (8) affect the result. Tools from the randomized algorithms (RAs) for control analysis framework (see [1] and references therein) can be used to evaluate the obtained (approximate) solutions. Let us denote the probability of constraint fulfillment for the first constraint in (8) by

$$p = \Pr\left[\|S(\boldsymbol{\theta}, \mathbf{k})\|_\infty - M_S \leq 0\right]. \tag{17}$$

The same approach presented here could be applied to any other probabilistic constraint. The RA framework provides estimates $\hat{p}$ of p, lying within an *a priori* specified accuracy $\epsilon \in (0, 1)$, with probability $1 - \delta$. This is formally stated as

$$\Pr\left[|p - \hat{p}| \leq \epsilon\right] \geq 1 - \delta. \tag{18}$$

A simple RA for constraint verification can be obtained through the MC method [1]. The constraint fulfillment probability estimates $\hat{p}$ are defined as

$$\hat{p} = \frac{1}{N} \sum_{i=1}^{N} \mathcal{I}\left[\|S(\boldsymbol{\theta}^{(i)}, \mathbf{k})\|_\infty - M_S\right], \tag{19}$$

where the samples $\boldsymbol{\theta}^{(1)}, \ldots, \boldsymbol{\theta}^{(N)}$ are generated by the PDF $f(\boldsymbol{\theta})$. A lower bound on the number of samples required to meet (18) is given by the Chernoff bound [1]

$$\frac{1}{2\epsilon^2} \log \frac{2}{\delta} \leq N. \tag{20}$$

A related analysis problem is to assess the worst-case constraint violation. That is, for a given δ and p^*, to obtain with probability $1 - \delta$, a level $\hat{\gamma}$ such that

$$\Pr\left[\|S(\boldsymbol{\theta}, \mathbf{k})\|_\infty \leq \hat{\gamma}\right] \geq p^*. \tag{21}$$

A simple RA for obtaining $\hat{\gamma}$ of (21) is

$$\hat{\gamma} = \max_{i=1,\ldots,N} \|S(\boldsymbol{\theta}^{(i)}, \mathbf{k})\|_\infty, \tag{22}$$

where $\boldsymbol{\theta}^{(1)}, \ldots, \boldsymbol{\theta}^{(N)}$ are, again, generated by the PDF $f(\boldsymbol{\theta})$ with a minimum number of samples given by

$$\frac{\log \delta}{\log p^*} \leq N. \tag{23}$$

It is remarkable that the previous lower bounds are independent of the dimension of the random variable $\boldsymbol{\theta}$. On the other hand, the number of samples becomes prohibitively high for obtaining very accurate estimates. That is why, we propose these techniques for analysis, but not for synthesis.

5 Examples

This section presents examples, illustrating the proposed method. The examples were obtained with the aid of a software package [21] to generate nodes and weights for the quadrature rules. Expectation integrals have been computed by using a sparse grid with dKP as underlying univariate quadrature. Estimates of constraint fulfillment probability $\hat{p}$ and worst-case constraint violation $\hat{\gamma}$ presented in the previous section are based on $\epsilon = \delta = 0.005$ for $\hat{p}$, and $\delta = 10^{-4}$ and $p^* = 1 - \delta$ for $\hat{\gamma}$.

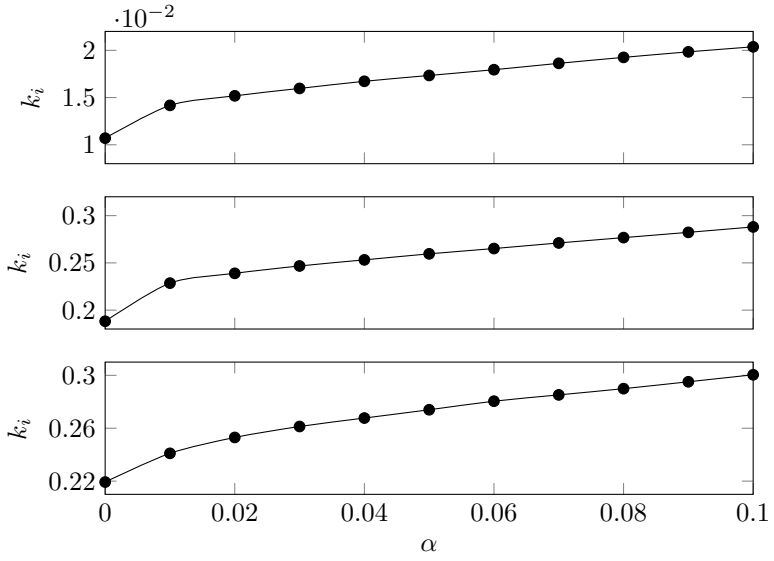

Figure 2: Optimal value of k_i according to (25) as function of α for for the processes P_1 (top), P_2 (middle), and P_3 (bottom).

5.1 Processes with different normalized time delay

This example considers three uncertain first-order time-delay (FOTD) processes: one lag dominant, one balanced, and one delay dominant:

$$P_1(s) = \frac{k}{s}e^{-hs}, \quad P_2(s) = \frac{k}{\tau s + 1}e^{-hs}, \quad P_3(s) = ke^{-hs}, \tag{24}$$

where $k \in [0.5, 1.5]$, $\tau \in [0.5, 1.5]$, and $h \in [0.5, 1.5]$. The controller (5) is considered for each of these uncertain processes. The time constant of the filter has been fixed to 0.1 s. (In practice the choice of the time constant of the filter will depend on the frequency content of the measurement noise.) The control design problem is formalized as follows:

$$\begin{aligned} \underset{\mathbf{k}=[k_p,k_i,k_d,0.1]^\top}{\text{minimize}} \quad & -k_i \\ \text{subject to} \quad & \Pr[\|S(\boldsymbol{\theta},\mathbf{k})\|_\infty \leq 1.4] \geq 1-\alpha_S, \\ & \Pr[\|T(\boldsymbol{\theta},\mathbf{k})\|_\infty \leq 1.4] \geq 1-\alpha_T. \end{aligned} \tag{25}$$

Fig. 2 shows the optimal value of k_i according to the design problem (25) as function of $\alpha = \alpha_S = \alpha_T$ for the uncertain processes presented in (24). These figures illustrate how allowing for a higher probability of constraint violation (by increasing the value of α) can significantly improve the level of performance in terms of maximizing k_i.

5.2 Comparison with alternative stochastic optimization design

This example contains a comparison with alternative stochastic design. It considers the following uncertain FOTD process model

$$P(s,\boldsymbol{\theta}) = \frac{1}{\tau s + 1}e^{-hs} \tag{26}$$

where $\boldsymbol{\theta} = [\tau, h]^\top$ with $\tau \in [0.5, 1.5]$ and $h \in [0, 0.5]$. This uncertain plant was considered in [12], where a PID controller was designed by solving the stochastic optimization problem:

$$\begin{aligned} \underset{\mathbf{k}=[k_p,k_i,k_d,0]^\top}{\text{minimize}} \quad & \mathbb{E}[\text{IAE}(\boldsymbol{\theta},\mathbf{k})] \\ \text{subject to} \quad & \max_{0\leq t\leq T} \mathbb{V}[y(t,\boldsymbol{\theta},\mathbf{k})] \leq D_y, \end{aligned} \tag{27}$$

Table 1: Comparison of controllers for the uncertain process model (26).

Method	k_p	k_i	k_d	IE	$\mathbb{E}$[IAE]
[12]	1.957	2.012	0.320	0.497	0.512
Proposed	0.807	1.150	0.132	0.870	0.955

Table 2: Probabilistic verification of controllers shown in Table 1.

Method	$1-\hat{p}_S$	$\hat{\gamma}_S$	$1-\hat{p}_T$	$\hat{\gamma}_T$
[12]	0.76	6.72	0.12	5.75
Proposed	0.05	1.54	0.00	1.24

where $\mathbb{V}[\cdot]$ denotes variance, and the value of D_y is a design specification. The solution was obtained by approximating the stochastic temporal response using polynomial chaos. The obtained controller, for $D_y = 0.01$ is shown in Table 1. We compare this controller with the one resulting from the following optimization problem

$$\begin{aligned} \underset{\mathbf{k}=[k_p,k_i,k_d,0]^\top}{\text{minimize}} \quad & -k_i \\ \text{subject to} \quad & \Pr[\|S(\boldsymbol{\theta},\mathbf{k})\|_\infty \leq 1.4] \geq 0.95, \\ & \Pr[\|T(\boldsymbol{\theta},\mathbf{k})\|_\infty \leq 1.4] \geq 0.95. \end{aligned} \tag{28}$$

The controller parameters obtained as solution to (28) are shown in Table 1, where the IE and average IAE values, the estimated probability of constraint violation of $\|S\|_\infty \leq 1.4$, and the estimated worst-case constraint violation of $\|S\|_\infty \leq 1.4$, are shown in Table 2. Load step responses are shown in Fig. 3.

The solution proposed in [12], in spite of considering uncertainty in the design stage, yields a very low level of robustness. Note that the worst cases of $\|S\|_\infty$ and $\|T\|_\infty$ are larger than 5 and acceptable values are in the interval $1.2-2$ [2]. Furthermore, the specification used in the problem (27) is not very intuitive. Although this constraint implicitly guarantees closed-loop stability in a probabilistic sense, it is difficult to associate values of D_y with values of any known stability margin.

5.3 Plant with large number of uncertain coefficients

This example illustrates that the proposed method is applicable in cases with more general parameter dependencies than intervals of transfer function coefficients, as in (3), and in cases with a large number of uncertain coefficients. The uncertain elastic two-mass system defined by the following transfer functions is considered (see Fig. 4):

$$P(s,\boldsymbol{\theta}) = \frac{c_s s + k_s}{d(s,\boldsymbol{\theta})}, \tag{29}$$

$$P_d(s,\boldsymbol{\theta}) = -\frac{J_m s^2 + (c_m + c_s)s + k_s}{d(s,\boldsymbol{\theta})}, \tag{30}$$

where

$$\begin{aligned} d(s,\boldsymbol{\theta}) =& J_m J_l s^3 + (J_l(c_m + c_s) + J_m(c_m + c_s))s^2 & (31)\\ &+ ((J_l + J_m)k_s + c_m c_l + c_m c_s + c_l c_s)s + (c_m + c_l)k_s. & (32) \end{aligned}$$

Here, $\boldsymbol{\theta} = [J_m, c_m, J_l, c_l, k_s, c_s]^\top$ denotes the vector of plant parameters. These two transfer functions represent the paths from plant input and disturbance, respectively, to plant output. The reader is referred to [25] for a more detailed description of this model. The following numerical values, taken from [25], are used in this example:

$$\begin{aligned} &J_m = 0.4 \text{ kg m}^2, && c_m \in [0, 0.1] \text{ Nm/(rad/s)}, \\ &J_l \in [5.5, 6.0] \text{ kg m}^2, && c_l \in [0, 1] \text{ Nm/(rad/s)}, \\ &k_s \in [3000, 4000] \text{ Nm/rad}, && c_s \in [1, 20] \text{ Nm/(rad/s)}. \end{aligned} \tag{33}$$

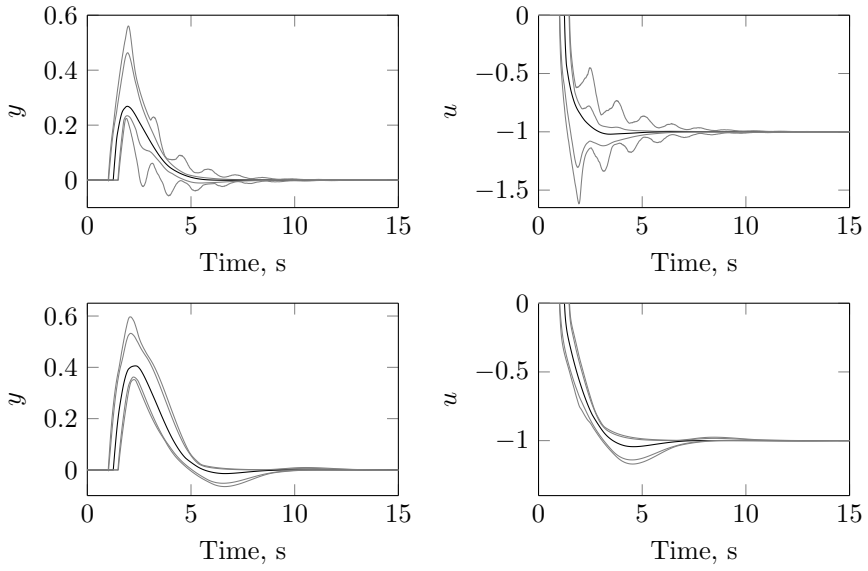

Figure 3: Plant output (left) and controller output (right) due to a unit step disturbance for the controller obtained in [12] (top) and the obtained with the proposed method (bottom). Black lines correspond to the median and gray lines correspond to 0.01, 0.05, 0.95, and 0.99 quantiles.

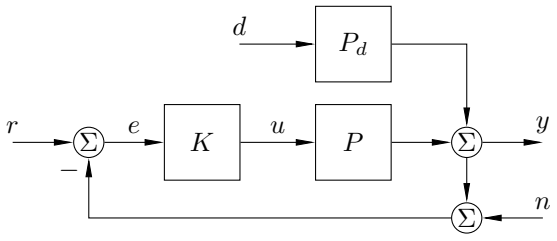

Figure 4: Feedback control system with the load disturbance entering through a model P_d.

Table 3: Solution to the design (35) for different values of α.

α	k_p	k_i	$1-\hat{p}_S$	$\hat{\gamma}_S$	$1-\hat{p}_T$	$\hat{\gamma}_T$
0.00	5.881	7.507	0.000	1.60	0.000	1.60
0.01	8.959	17.981	0.010	2.29	0.005	1.61
0.02	10.448	24.634	0.020	2.98	0.013	1.99

Although the disturbance acts on the output through P_d, minimization of the corresponding IE is equivalent to maximization of k_i:

$$\text{IE} = \int_0^\infty e(\tau, \boldsymbol{\theta}, \mathbf{k}) d\tau = \lim_{s\to 0} s \frac{P_d(s)}{1+P(s)K(s)} \frac{1}{s^2} = -\frac{1}{k_i}. \tag{34}$$

A PI is often used for these kind of system, in particular, when actuator dynamic (including delays) is relatively slow, since it limits the advantage of high bandwidth controllers [25]. This motivates the problem formulation:

$$\begin{aligned} \underset{\mathbf{k}=[k_p,k_i,0,0]^\top}{\text{minimize}} \quad & -k_i \\ \text{subject to} \quad & \Pr[\|S(\boldsymbol{\theta},\mathbf{k})\|_\infty - 1.6 \le 0] \ge 1-\alpha_S, \\ & \Pr[\|T(\boldsymbol{\theta},\mathbf{k})\|_\infty - 1.6 \le 0] \ge 1-\alpha_T. \end{aligned} \tag{35}$$

Table 3 shows the solution to (35) for different values of $\alpha = \alpha_S = \alpha_T$. Estimates of the probability of constraint violation and worst-case specification are also shown. In this example, the level of performance increases considerably even for small (e.g. $1-2$ %) probabilities of constraint violation. The estimated PDF of $\|S\|_\infty$ and $\|T\|_\infty$ are shown in Fig. 5 and 6.

Finally, it is worth mentioning that, in this example, the computational time required by using sparse grid with dKP is shorter, by a factor of 10, than the one required by full grid with GL. This fact makes the full grid approach impractical for high-dimensional problems.

6 Discussion

6.1 Summary

This paper has presented an approach for cost, constraint and associated gradient computations, arising when solving robust PID synthesis problems, of the type (2), for plants with parametric uncertainties. The actual optimization is assumed to be handled by a solver, utilizing these computations.

Evaluating the mentioned cost, constraints and associated gradients, relies on the evaluation of multivariate expectation integrals, of the form (11). In general, they cannot be exactly evaluated, introducing the need of numerical approximation methods. We study a class of such methods for the univariate case, known as nested quadrature rules, which enables an extension to the multivariate case using Smolyak's product, without the exponential complexity associated with the naive (full-grid) approach.

The effectiveness of the proposed approach is demonstrated through realistic PID synthesis examples. These examples show that a slight relaxation of constraint fulfillment probability, can serve to increase performance significantly. I.e., considering only the worst case is often conservative.

The approximations associated with sparse grid quadrature and sigmoid approximation of the indicator function are verified to be sound, by means of the randomized algorithms (RAs) framework.

6.2 Conclusions

The main conclusion is that the use of sparse-grid methods, based on combining Smolyak's product with nested univariate quadrature rules, constitutes a feasible approach to evaluating the integrals necessary for solving robust controller synthesis problems for plants with parametric uncertainties. This has been demonstrated through examples, for which the introduced approximations were demonstrated to be sound, using randomized algorithms.

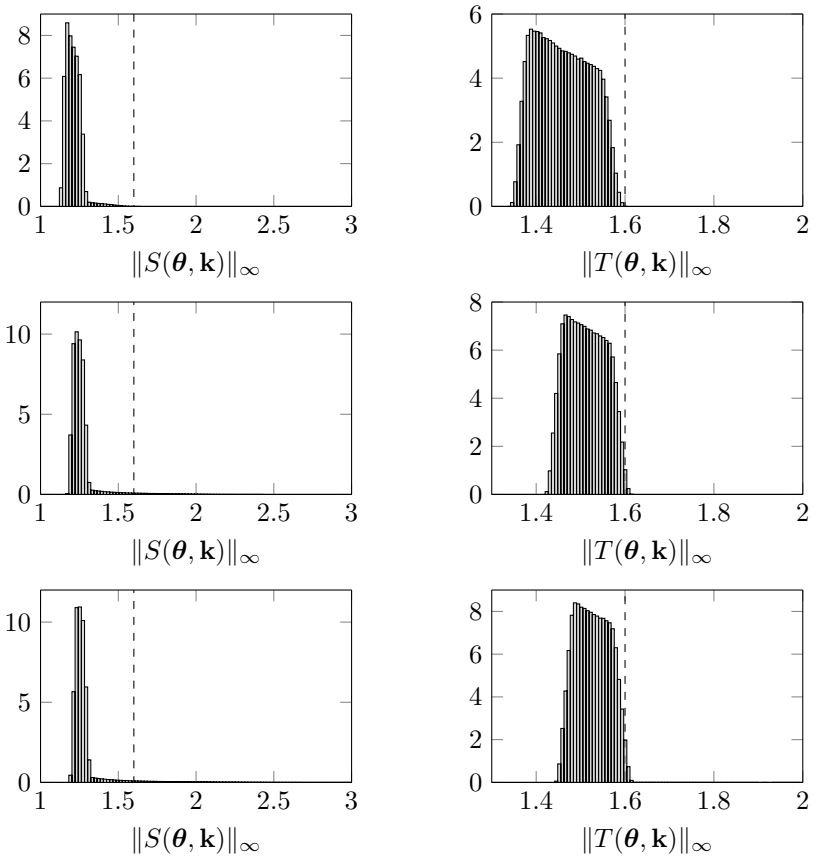

Figure 5: Probability density functions of $\|S(\boldsymbol{\theta}, \mathbf{k})\|_\infty$ and $\|T(\boldsymbol{\theta}, \mathbf{k})\|_\infty$ for the controllers presented in Table 3. Top, middle, and bottom correspond to $\alpha = 0.00, 0.01$, and 0.02, respectively.

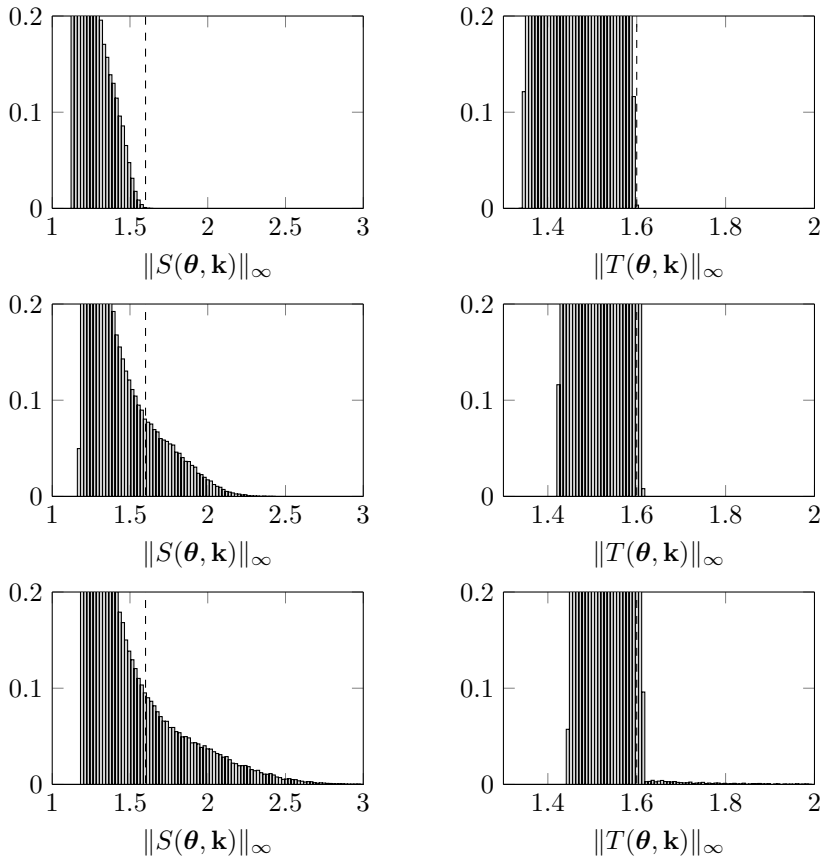

Figure 6: Details of the probability density functions shown in Fig. 5. Top, middle, and bottom correspond to $\alpha = 0.00, 0.01$, and 0.02, respectively.

Relatedly, it can be noted that significant performance gains can be made, if probabilities $\alpha > 0$ for constraint violations are permitted. For instance, the last example shows how performance can be tripled by allowing for constraint violation with a probability of 2 %. The approach of probabilistically relaxing constraint satisfaction comes even more natural when uncertainties are described by distributions with infinite tails, for which there exist no worst case. This is true for instance when the parameter vector follows a multivariate Gaussian distribution, as was studied in [11].

The two main limitation of the proposed approach, which are rather properties of local optimization methods than the suggested quadrature approximation, are the need of a feasible initial point and the lack of guarantees to attain a global minimum.

Acknowledgment

This work has been supported by Ministerio de Economía e Innovación of Spain under project DPI2013-47100-C2-1-P (including FEDER co-funding). The first author is also supported by an FPU grant (FPU12/01026) from the Ministerio de Educación, Cultura y Deporte of Spain. The second author would like to acknowledge the LCCC and ELLIIT research centra at Lund University.

References

References

[1] R. Tempo, G. Calafiore, F. Dabbene, Randomized algorithms for analysis and control of uncertain systems: with applications, Springer, 2012.

[2] K. J. Åström, H. Panagopoulos, T. Hägglund, Design of PI controllers based on non-convex optimization, Automatica 34 (5) (1998) 585–601.

[3] K. J. Åström, T. Hägglund, Advanced PID control, ISA-The Instrumentation, Systems, and Automation Society, 2006.

[4] M. Hast, K. J. Åström, B. Bernhardsson, S. Boyd, PID design by convex-concave optimization, in: European Control Conference, Zurich, Switzerland, 2013, pp. 4460–4465.

[5] P. Mercader, K. J. Åström, A. Baños, T. Hägglund, Robust PID design based on QFT and convex-concave optimization, IEEE Transactions on Control Systems Technology 25 (2) (2017) 441–452.

[6] O. Garpinger, T. Hägglund, K. J. Åström, Performance and robustness trade-offs in PID control, Journal of Process Control 24 (5) (2014) 568–577.

[7] C. Grimholt, S. Skogestad, Improved optimization-based design of PID controllers using exact gradients, in: European Symposium on Computer Aided Process Engineering, Copenhagen, Denmark, 2015.

[8] K. Soltesz, C. Grimholt, S. Skogestad, Simultaneous design of proportional–integral–derivative controller and measurement filter by optimisation, IET Control Theory & Applications 11 (3) (2017) 341–348.

[9] E. Boje, Quantitative feedback design for systems with probabilistic parameterizations, International Journal of Robust and Nonlinear Control 17 (2–3) (2007) 173–179.

[10] P. Mercader, K. Soltesz, A. Baños, PID syntehsis under probabilistic parametric uncertainty, in: American Control Conference, Boston, USA, 2016, pp. 5467–5472.

[11] K. Soltesz, P. Mercader, A. Baños, An automatic tuner with short experiment and probabilistic plant parameterization, International Journal of Robust and Nonlinear Control 27 (11) (2017) 1857–1873.

[12] P. L. T. Duong, M. Lee, Robust PID controller design for processes with stochastic parametric uncertainties, Journal of Process Control 22 (9) (2012) 1559–1566.

[13] C. Wang, D. Li, Decentralized PID controllers based on probabilistic robustness, Journal of Dynamic Systems, Measurement, and Control 133 (6) (2011) 061015.

[14] S. Panda, B. Sahu, P. Mohanty, Design and performance analysis of PID controller for an automatic voltage regulator system using simplified particle swarm optimization, Journal of the Franklin Institute 349 (8) (2012) 2609–2625.

[15] A. Hajiloo, N. Nariman-Zadeh, A. Moeini, Pareto optimal robust design of fractional-order PID controllers for systems with probabilistic uncertainties, Mechatronics 22 (6) (2012) 788–801.

[16] C. Yeroğlu, A. Ateş, A stochastic multi-parameters divergence method for online auto-tuning of fractional order PID controllers, Journal of the Franklin Institute 351 (5) (2014) 2411–2429.

[17] B. Barmish, C. M. Lagoa, The uniform distribution: A rigorous justification for its use in robustness analysis, Mathematics of Control, Signals and Systems 10 (3) (1997) 203–222.

[18] J. Nocedal, S. Wright, Numerical optimization, Springer, 2006.

[19] H.-J. Bungartz, M. Griebel, Sparse grids, Acta numerica 13 (2004) 147–269.

[20] K. Petras, Smolyak cubature of given polynomial degree with few nodes for increasing dimension, Numerische Mathematik 93 (4) (2003) 729–753.

[21] F. Heiss, V. Winschel, Likelihood approximation by numerical integration on sparse grids, Journal of Econometrics 144 (1) (2008) 62–80.

[22] S. A. Smolyak, Quadrature and interpolation formulas for tensor products of certain classes of functions, Soviet Mathematics Doklady 4 (1963) 240–243.

[23] G. W. Wasilkowski, H. Wozniakowski, Explicit cost bounds of algorithms for multivariate tensor product problems, Journal of Complexity 11 (1) (1995) 1–56.

[24] V. N. Vapnik, An overview of statistical learning theory, IEEE Transactions on Neural Networks 10 (5) (1999) 988–999.

[25] M. Nordin, P.-O. Gutman, Controlling mechanical systems with backlash – a survey, Automatica 38 (10) (2002) 1633–1649.